Structural precursor to the metal-insulator transition in V_2O_3

P. Pfalzer, G. Obermeier, M. Klemm, and S. Horn

Institut für Physik, Universität Augsburg, Universitätsstrasse 1, 86159 Augsburg, Germany

M. L. denBoer

Queens College of CUNY, 65-30 Kissena Boulevard, Flushing, New York 11367, USA

The temperature dependence of the local structure of V_2O_3 in the vicinity of the metal-to-insulator transition (MIT) has been investigated using hard x-ray absorption spectroscopy. It is shown that the vanadium pair distance along the hexagonal c axis changes abruptly at the MIT as expected. However, a continuous increase of the tilt of these pairs sets in already at higher temperatures and reaches its maximum value at the onset of the electronic and magnetic transition. These findings confirm recent theoretical results which claim that electron-lattice coupling is important for the MIT in V_2O_3. Our results suggest that the distortion of the symmetry of the basal plane plays a decisive role for the MIT and orbital degrees of freedom drive the MIT via changes in hybridization.

I. INTRODUCTION

The metal-to-insulator transition in (MIT) V_2O_3 is a long standing yet not completely resolved issue. Originally being discussed as the classical example of a Mott-Hubbard transition,[1] this interpretation has to be questioned due to the intimate interplay of structural, electronic and magnetic changes in the phase diagram of this compound.[2] Therefore it is not clear whether electronic correlations can completely account for the MIT in V_2O_3 or if structural effects play an important role. The relevance of possible electron-lattice interactions has been stressed by recent theoretical work.[3,4]

In an earlier paper[5] we have shown that a detailed understanding of the interplay of structural and electronic degrees of freedom requires both information on the global structure as measured by x-ray diffraction (XRD) and of the local structure of the compound. Interatomic distances and symmetries can deviate locally from the global lattice symmetry, therefore indicating the presence of an order-disorder component of the transitions or of structural fluctuations. Our earlier results demonstrate that the two insulating phases of V_2O_3, the paramagnetic insulating (PI) and the antiferromagnetic insulating (AFI) phase, are structurally very similar on a local scale and therefore indicate that there might exist a common route for both the transitions from the paramagnetic metallic (PM) phase to the PI and the AFI phase, respectively.

In this paper, we investigate the evolution of the local structure of V_2O_3 in the vicinity of the PM to AFI transition to shed light on the detailed structural changes associated with the MIT. The results of our temperature dependent extended x-ray absorption fine structure (EXAFS) measurements show a rather complex behavior of the local structure, which differs along different crystallographic axes. In particular, we observe a structural precursor to the MIT which consists of characteristic changes of nearest neighbor distances.

II. EXPERIMENT

EXAFS measurements were performed on a V_2O_3 single crystal grown by chemical transport using $TeCl_4$ as the transport agent. The crystal was mounted on a thin glass plate and reduced in thickness by lapping and polishing the sample down to approximately 12 μm which corresponds to roughly two absorption lengths. This treatment allowed one to detect the x-ray absorption in a transmission geometry, thereby avoiding damping of the signal due to self-absorption effects which would have been present in fluorescence mode.[6] The sample was oriented so that the angle between the polarization vector E of the incoming x-rays and the hexagonal c axis of the crystal (c_{hex}) could be changed by rotating the sample around the surface normal. Measurements were made with E parallel and perpendicular to c_{hex}. This procedure allows one to separate scattering paths along and perpendicular to the hexagonal c axis as detailed in Ref. 5.

The electrical resistivity was measured using a standard four-probe dc technique. For each measurement the current was reversed to eliminate offsets. Contacts were made by attaching platinum wires (diameter: 40 μm) to the sample by silver epoxy. Metallic behavior was observed in the high temperature region, and a sharp jump in the resistance of more than three orders of magnitude at a temperature of 140 K signaled the MIT.[7] The slightly reduced transition temperature indicates that a small vanadium deficiency occurred during the growth of the single crystal. The magnetic transition from PM to AFI occurred in a temperature region from 140 K down to 130 K as determined by magnetic susceptibility measurements using a Quantum Design superconducting quantum interference device (SQUID) magnetometer.

EXAFS measurements at the vanadium K edge (5465 eV) were performed at beam line X23B of the National Synchrotron Light Source at Brookhaven National Laboratory. Spectra at different temperatures above, at, and below the transition temperature were taken using a closed cycle helium
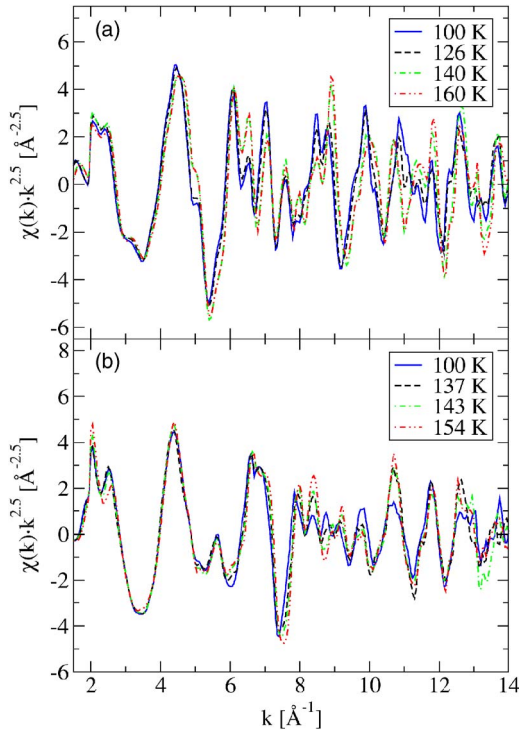
FIG. 1. (Color online). EXAFS spectra of the V K edge of V_2O_3 in the vicinity of the MIT at $T=140$ K. The spectra in a geometry with E parallel to c_{hex} are almost identical within one phase and display an abrupt change at the MIT (a). Only smooth changes are observed in a setup where E is perpendicular to c_{hex} (b).
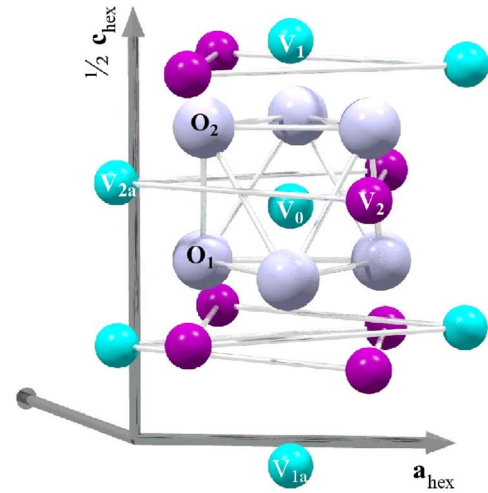

FIG. 2. (Color online). Room temperature structure of V_2O_3. Small (large) spheres represent vanadium (oxygen) ions. Only those oxygen ions which form an octahedron around the central vanadium ion V_0 are shown. Vanadium ions which have opposite spin in the AFI phase are drawn in different colors.

cryostat. The sample was held under vacuum to avoid water condensation and to reduce heat transmission. As no temperature sensor was available in the direct neighborhood of the sample, the resistivity of the crystal was monitored *in situ* during the EXAFS experiment in the geometry with E perpendicular to c_{hex}. This allowed for a direct observation of the metal to insulator transition itself. The electronic transition was observed at a temperature of 130 K at the cold finger of the cryostat. The temperature difference of −10 K compared to the *ex situ* resistance measurements can be attributed to a temperature gradient between the cold finger and the sample. Temperatures given in the paper are corrected accordingly.

The crystal has been examined by XRD measurements after the EXAFS experiments were finished. The investigations, both in $\Theta/2\Theta$ and in Laue geometries, confirmed that the MIT did not destroy the single crystal, as the diffraction patterns were those expected for a good single crystal and no signs of twinning could be observed. In addition, spectra above the transition were measured before and after the crystal passed through the MIT during the EXAFS experiment. No differences were observed in these spectra, ruling out the influence of possible cracks on the measurements as well. Typcial spectra are shown in Fig. 1 and display that a good signal-to-noise ratio could be achieved at least up to a wave vector of $k=14$ Å^{-1} (k being the wave vector of the outgoing photoelectron).

Standard EXAFS analysis using the ATHENA[8] and IFEFFIT[9] programs was performed to extract path lengths and other

parameters from the spectra. The experimental spectra were normalized to the edge step and a smooth, atomiclike background was subtracted by minimizing the low-R contribution in the Fourier-transformed data.[10] The EXAFS equation in cumulant expansion as defined in Ref. 11 and implemented in the IFEFFIT program was used up to the third cumulant C_3 to fit the experimental data to model spectra calculated with FEFF8.2.[12] For the Fourier transforms a window in k space from 2 to 13 Å was used and the spectra were weighted by $k^{2.5}$. Fitting was carried out in real space in a range from 1.2 to 4.1 Å ($E\|c_{hex}$) and from 1.2 to 3.65 Å ($E\perp c_{hex}$), respectively. The cluster of ions used for the calculation of the model spectra was derived from the lattice parameters and atomic positions resulting from XRD measurements for the trigonal structure of V_2O_3 at room temperature published in Ref. 13.

The structure refinement was performed by varying the interatomic distances to all vanadium ions up to a shell radius of 4.3 Å, which corresponds to the V ions shown in Fig. 2. In addition, backscattering from the six oxygen ions that form the coordination octahedron of the absorber was accounted for. Inclusion of the second backscattering shell of oxygen ions improved the quality of the fit, but had no influence on the fitting parameters concerning the ions shown in Fig. 2. At the transition from the paramagnetic metal to the antiferromagnetic insulator, the lattice symmetry reduces from trigonal to monoclinic. Comparing the interatomic distances of the trigonal and the monoclinic structure as calculated from the data published in Refs. 13–16 and summarized in the two rightmost columns of Table I, it turns out that the transition increases the distance of the neighboring vanadium ions along the hexagonal c axis(V_0 and V_1) by 0.04 Å. In addition, the threefold symmetry in the plane perpendicular to c_{hex} (the basal plane) is broken and one of the three vanadium neighbors in this plane (V_{2a}) increases its distance to the absorber (V_0) by 0.11 Å, while the distance to the two other V_2 ions remains nearly constant.

TABLE I. Definition of the next neighbor V-V distances in the fitting model. The free parameters are $dv1$ for the change ($R_{monoclinic} - R_{trigonal}$) of the V_0-V_1 distance and $dv2$ for the change of the V_0-V_{2a} distance, respectively. The changes ΔR of the remaining V-V distances used in the fits with with $\boldsymbol{E}\|\boldsymbol{c}_{hex}$ and with $\boldsymbol{E}\perp\boldsymbol{c}_{hex}$ are set as multiples of these values to represent the values calculated from the trigonal and monoclinic structure as measured by XRD (right columns) when $dv1$ and $dv2$ take on the respective values of $dv1 = 0.04$ Å and $dv2 = 0.11$ Å.

| | ΔR | | $R_{trigonal}$ | $R_{monoclinic}$ |
	$\boldsymbol{E}\|c_{hex}$	$\boldsymbol{E}\perp\boldsymbol{c}_{hex}$		
V_0-V_1	$dv1$		2.70	2.74
V_0-V_{2a}		$dv2$	2.88	2.99
V_0-V_{2b}		0	2.88	2.88
V_0-V_{2c}		$-2/11\cdot dv2$	2.88	2.86
V_0-V_{3a}	$-3/4\cdot dv1$	$-3/11\cdot dv2$	3.47	3.44
V_0-V_{3b}	$-1/4\cdot dv1$	$-1/11\cdot dv2$	3.47	3.46
V_0-V_{4a}	$-6/4\cdot dv1$	$-6/11\cdot dv2$	3.69	3.63
V_0-V_{4b}	$4/4\cdot dv1$	$4/11\cdot dv2$	3.69	3.73
V_0-V_{4c}	$5/4\cdot dv1$	$5/11\cdot dv2$	3.69	3.74
V_0-V_{1a}	$-7/4\cdot dv1$		4.30	4.23

To allow for this monoclinic distortion in the fitting model, the distance between the absorber and these V neighbors (V_1 for the spectra with $\boldsymbol{E}\|\boldsymbol{c}_{hex}$ and V_{2a} for the spectra with $\boldsymbol{E}\perp\boldsymbol{c}_{hex}$) was allowed to vary freely, while the distances to the remaining V ions were given as multiples of this value as defined in Table I. This allowed us to describe the changes of all V-V distances with a single parameter for each orientation ($dv1$ or $dv2$). In the same way the positions of the O ions were split up as multiples of $dv1$ and $dv2$, respectively. An additional isotropic change of the V-O distances was allowed to account for a possible change in the oxygen positions due to the vanadium deficiency of the crystal. A damping term (Debye-Waller factor) was assigned to each neighboring shell, and for the nearest vanadium neighbors the third cumulant was used as an additional free parameter. Altogether, 12 free parameters were used. The maximum number of variables that can be fitted is given by $N_{idp} = 2\Delta k \Delta R/\pi$, where Δk and ΔR are the range of wave vectors k and interatomic distances R included in the fit. N_{idp} amounts to approximately 16 variables per spectra for the present study.

III. RESULTS

All measured spectra could be fitted successfully with a reliability factor of less than 0.02, indicating that the model was well suited to describe the data. For temperatures slightly below and above the MIT, the Fourier-transforms of four spectra and the respective fits are shown in Fig. 3. The values for the reliability factors and reduced chi-squared for the fits are compiled in Table II.

Figures 4 and 5 show the fit results for the scattering paths to the next vanadium neighbors along (V_1) and perpendicular (V_2, V_{2a}) to the hexagonal c axis. The geometry used in the measurement allowed for a separation of these paths: Backscattering from the V_1 neighbor only occurs in the spectra with $\boldsymbol{E}\|\boldsymbol{c}_{hex}$, while the V_2 and V_{2a} backscatterers only contribute to the spectra with $\boldsymbol{E}\perp\boldsymbol{c}_{hex}$. The Fourier transformed spectra show a well separated structure located between 2 and 3 Å (see Fig. 3). This structure is attributed to single scattering contributions either of the V_1 or the V_2, V_{2a} scattering paths, only. Therefore no correlations between fit variables of these paths can occur, although the distance from the absorber V_0 to all of these neighbors is similar.

Figure 4(a) clearly shows that the distances between the next V neighbors along the hexagonal c axis correspond to the values expected from XRD results: The distance in the AFI phase at low temperatures is about 0.04 Å larger than in the high temperature PM phase. The change is abrupt as a function of temperature and occurs in a temperature window corresponding to that of the change in magnetic susceptibility. The measurement uncertainty of the V_0-V_1 distances amounts to ≈ 0.01 Å. The Debye-Waller factor σ^2, shown in Fig. 5(a), exhibits a sharp rise at the onset of the MIT, indicating either large fluctuations or a static distribution of widely varying distances while the magnetic transition occurs.

The next neighbor distances in the basal plane display a very different behavior. First of all the distance from the absorber ion V_0 to the V_{2a} neighbor is larger than expected from XRD in the high temperature PM phase [see Fig. 4(b)], i.e., larger than the V_0-V_2 distances. This break of the threefold symmetry expected from the long range structure probed by XRD corresponds to a monoclinic symmetry. The elongation of the V_0-V_{2a} distance, which could be determined with an accuracy of ≈ 0.02 Å, measures the size of this monoclinic distortion. In the PM phase it is reduced to about 30% of the distortion in the AFI phase, as was first observed in Ref. 17. The transition to the full monoclinic distortion in the basal plane is much broader in temperature than that observed for the V-V distance along the hexagonal c axis. The onset occurs in a region well above the electronic and magnetic transitions. This is consistent with the fact that
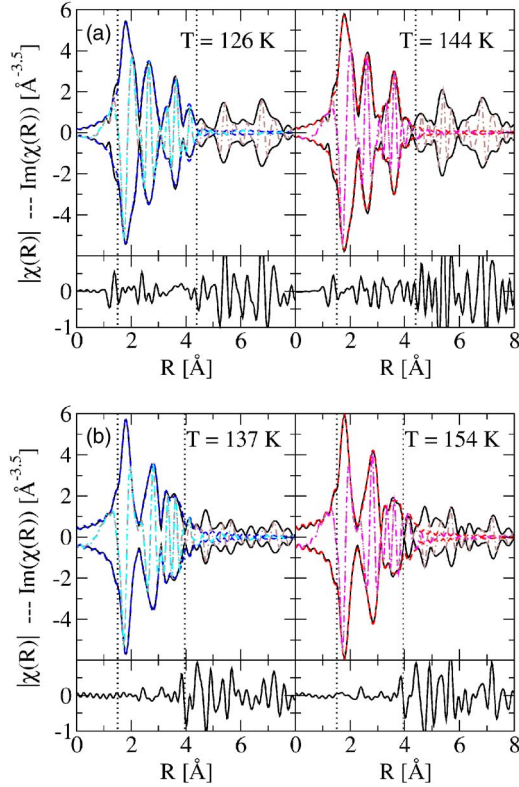
FIG. 3. (Color online). Typical examples of the Fourier transformed EXAFS spectra of V_2O_3 at temperatures close to the MIT in a geometry with E parallel to c_{hex} (a) and with E perpendicular to c_{hex} (b). Solid and dash-dotted lines represent the amplitude and imaginary part of the Fourier transformed data, dashed and double-dotted dashed lines show the fitted model spectra. Data and fit coincide well in the fitting range (marked by vertical dotted lines) as can be seen from the difference spectra of the imaginary parts of data and fit in the respective lower panels. For this figure, the scattering phase shift of the central V ion has been corrected, which basically leads to a shift of the fourier transformed spectra and the fitting ranges to the right by ≈ 0.3 Å.

the Debye-Waller factor of the in-plane V neighbors [Fig. 5(b)] does not show a significant change at the MIT.

Third cumulants (C_3 or $\sigma^{(3)}$) which account for the anisotropy of the scattering paths to the next V neighbors where found to have a significant influence on the spectra in the low temperature AFI phase, but are negligible in the PM phase. The third cumulants show only a weak temperature dependence in the AFI phase and adopt values of ≈ -0.0003 Å^3 for the V_0-V_1 scattering path and ≈ -0.0007 Å^3 for the V_0-V_2 and V_0-V_{2a} scattering paths, respectively. The error is estimated to approximately $\pm 25\%$.

Distances between the central vanadium ion V_0 and the oxygen ions forming its coordination octahedron did not deviate from the values expected from XRD within error bars, i.e., these vanadium-oxygen distances remain nearly constant throughout the whole temperature range.

Summarizing, we can characterize the structural evolution at the metal-to-insulator transition of V_2O_3 as follows: Structural changes along the hexagonal c axis are restricted to a sharply bounded temperature range given by the MIT. Perpendicular to c_{hex}, however, the tilt of the c-axis V pairs, indicated by the elongation of the V_0–V_{2a} bond, starts to increase already far above the MIT.

IV. DISCUSSION

Precursor effects to the MIT in V_2O_3 have already been observed in electrical resistance under pressure[18] and very

TABLE II. r-factors and reduced chi-squared (χ_ν^2) for the fits presented in Figs. 3–5.

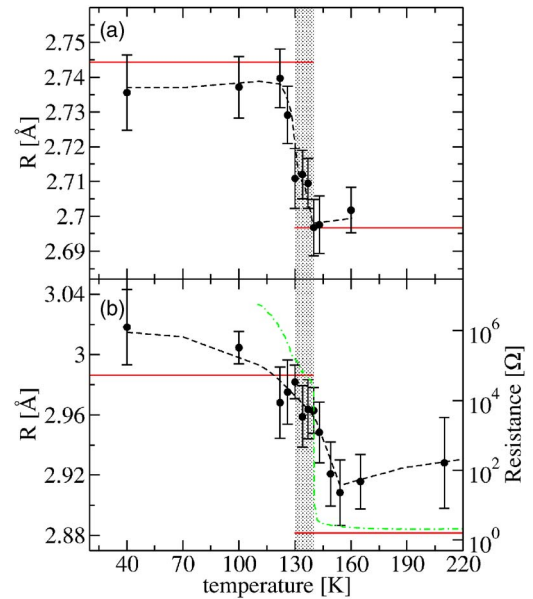| Temperature (K)	$E \parallel c_{hex}$		$E \perp c_{hex}$	
	r-factor	χ_ν^2	r-factor	χ_ν^2
40	0.020	197	0.004	56
100	0.014	121	0.001	18
122	0.014	25	0.006	17
126	0.010	52	0.006	37
130	0.009	47	0.002	7
134	0.006	29	0.005	28
137	0.007	24	0.005	46
140	0.012	43	0.003	24
143	0.013	58	0.004	33
149			0.004	30
154			0.003	34
160	0.007	17		
165			0.003	21
210			0.007	30

FIG. 4. (Color online). Temperature dependence of the distances of the V_0-V_1 (a) and V_0-V_{2a} (b) scattering paths as resulting from the fits to the EXAFS spectra (dots). Solid lines represent the distances expected from XRD. The dash-dotted line in (b) shows the result of the *ex situ* resistance measurement. The shaded temperature range marks the range of the magnetic transition. Dashed lines through the fit results provide a guide to the eye.
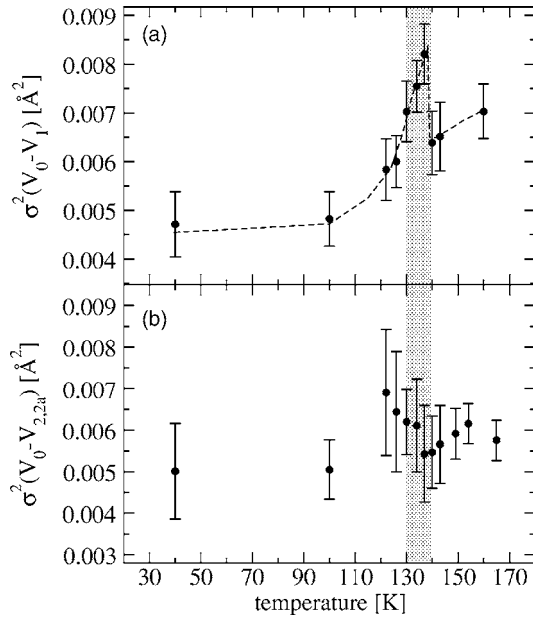
FIG. 5. Temperature dependence of the Debye-Waller factors σ^2 for the V_0-V_1 (a) and V_0-$V_{2,2a}$ (b) scattering paths as resulting from the fits to the EXAFS spectra. Like in Fig. 4, the shaded temperature range marks the range of the magnetic transition. The dashed line through the fit results provides a guide to the eye.

recently in the sound velocity measured for thin films.[19] The results of our local structure determination show for the first time that structural changes preceed the changes in transport and magnetic properties.

The analysis of the polarization dependent measurements reveals that two distinct movements with different temperature dependencies have to be distinguished: The positioning of the vanadium ions within the basal plane and the change of the V-V pair distance perpendicular to the basal plane, i.e., along the hexagonal c axis. The former movement determines the rotation of these vanadium pairs, ranging from an alignment parallel to c_{hex} in the PM phase to a tilt of roughly 2° away from this axis in the AFI phase.[15]

Following Tanaka,[3] hybridization between the a_{1g} and the e_g^π orbitals increases on rotating the V_0-V_1 pairs out of the direction of the c axis. Depending on the hybridization strength, two minima of the free energy exist, which are characterized by two different equilibrium distances between the two nearest V neighbors along c_{hex}. While the electron-lattice coupling is weak when the V-V pair is aligned parallel to the hexagonal c axis, increased hybridization on tilting the pair renders the possible V $3d$ orbital configurations almost energetically degenerate. The so modified interactions favor a new ground state configuration with a reduced occupation of the a_{1g} orbital.[20,21] In this configuration, the electron-lattice coupling is strong and an enlarged V pair distance is expected.

We observe a continuously increasing tilt, starting well above the MIT and continuing even within the AFI phase. Along with it, the hybridization strength increases as just pointed out. At a certain hybridization strength, the system snaps into the second minimum of the free energy, which corresponds to the enlarged pair distance. Therefore it is

plausible that the V_0-V_1 distance expands primarily after the tilt of the pair has adopted its maximum value, which is exactly the behavior we observe experimentally. Our measurements thereby substantiate the scenario proposed by Tanaka which does not regard the metal-insulator transitions in V_2O_3 (both the PM to AFI and the PM to PI transitions) as usual Mott transitions.[3] The fact, that on a local scale the trigonal symmetry is not fully recovered in the metallic phase, suggests that the trigonal and monoclinic structure are very close in energy, allowing fluctuations between the two. We want to point out that the present results are consistent with our earlier findings[5] that the trigonal symmetry can be broken on a local scale while the global symmetry remains trigonal.

In step with the separation of the two neighboring V ions along the hexagonal c axis an "umbrella like" distortion of the oxygen coordination octahedron around each V ion occurs.[22] Thus the trigonal distortion of the coordination octahedron is directly determined by the distance between the next V neighbors along c_{hex}. The increased distortion of the oxygen octahedron is responsible for the stabilization of the insulating state[4] since it results in a large shift of (dynamical) spectral weight.

However, from theoretical considerations it has been pointed out[23] that in-plane interactions are important for the MIT in V_2O_3 and should not be treated as small perturbations. While our measurements cannot unambiguously distinguish if V-V in-plane interactions, interactions between vanadium ions and their next oxygen neighbors, or a combination of the two cause the increase of the tilt of the V_0-V_1 pair, they clearly show that the distortion of the trigonal symmetry is a decisive ingredient to the MIT by triggering the modification of the V_0-V_1 distance via changes in hybridization. Similar results have been derived earlier for the local symmetry of the PI phase, which corresponds to the monoclinic structure of the AFI phase.[5]

In this context it is interesting to note that the Debye-Waller factor of the in-plane vanadium neighbors does not display substantial changes at the transition. If structural degrees of freedom were the driving force behind the increase of the in-plane interatomic distances, the Debye-Waller factor should be strongly affected. A possible explanation could be that the change in hybridization is driven by orbital interactions. The change in hybridization will also result in a change of the crystal field splitting and accordingly alter the orbital occupation. Evidence for orbital interactions is given from neutron scattering results by Bao *et al.*[24] As shown by Laad *et al.*, the variation of orbital occupation can result in a first order phase transition.[25]

V. CONCLUSION

In conclusion, the measurements of the local structure of pure V_2O_3 in the vicinity of the metal-to-insulator transition show that complex changes of the interatomic distances on a local scale are decisive for the changes of the physical properties at the transition. We can distinguish between two structural effects with different temperature characteristics: At the onset of the electronic and magnetic transition temperature,

the next vanadium neighbors along the hexagonal *c* axis abruptly increase their distance, resulting in an increase of the trigonal crystal field component and a shift of spectral weight, rendering the system insulating. However, a continuous increase of the monoclinic distortion in the basal plane is already observed far above the MIT reaching its maximum value at the onset of the electronic and magnetic transition. While the monoclinic distortion, in other words the tilt of the *c*-axis vanadium pair against this axis, determines the orbital configuration via changes in hybridization strength, the pair distance only reacts to these changes by locking into one of the two minima of the free energy defined by the orbital configuration. These findings suggest that orbital degrees of freedom drive the metal-to-insulator transition via changes in hybridization triggered by the distortion of the trigonal symmetry in the basal plane.

[1] D. B. McWhan, T. M. Rice, and J. P. Remeika, Phys. Rev. Lett. **23**, 1384 (1969).

[2] D. B. McWhan, A. Menth, J. P. Remeika, W. F. Brinkman, and T. M. Rice, Phys. Rev. B **7**, 1920 (1973).

[3] A. Tanaka, J. Phys. Soc. Jpn. **71**, 1091 (2002).

[4] M. S. Laad, L. Craco, and E. Müller-Hartmann, Phys. Rev. B **73**, 045109 (2006).

[5] P. Pfalzer, J. Will, A. Nateprov, Jr., M. Klemm, V. Eyert, S. Horn, A. I. Frenkel, S. Calvin, and M. L. denBoer, Phys. Rev. B **66**, 085119 (2002).

[6] P. Pfalzer, J.-P. Urbach, M. Klemm, S. Horn, M. L. denBoer, A. I. Frenkel, and J. P. Kirkland, Phys. Rev. B **60**, 9335 (1999).

[7] All temperatures given in this paper are measured on cooling.

[8] B. Ravel and M. Newville, J. Synchrotron Radiat. **12**, 537 (2005).

[9] M. Newville, J. Synchrotron Radiat. **8**, 322 (2001).

[10] M. Newville, P. Livins, Y. Yacoby, J. J. Rehr, and E. A. Stern, Phys. Rev. B **47**, 14126 (1993).

[11] M. Newville, B. Ravel, D. Haskel, J. J. Rehr, E. A. Stern, and Y. Yacoby, Physica B **208&209**, 154 (1995).

[12] A. L. Ankudinov, C. E. Bouldin, J. J. Rehr, J. Sims, and H. Hung, Phys. Rev. B **65**, 104107 (2002).

[13] M. G. Vincent, K. Yvon, and J. Ashkenazi, Acta Crystallogr., Sect. A: Cryst. Phys., Diffr., Theor. Gen. Crystallogr. **A36**, 808 (1980).

[14] D. B. McWhan and J. P. Remeika, Phys. Rev. B **2**, 3734 (1970).

[15] P. D. Dernier and M. Marezio, Phys. Rev. B **2**, 3771 (1970).

[16] L. D. Calvert and P. Villars, *Pearson's Handbook of Crystallographic Data for Intermetallic Phases*, Vol. 4 (ASM International, Metals Park, Ohio 1991).

[17] A. I. Frenkel, E. A. Stern, and F. A. Chudnovsky, Solid State Commun. **102**, 637 (1997).

[18] S. A. Carter, T. F. Rosenbaum, M. Lu, H. M. Jaeger, P. Metcalf, J. M. Honig, and J. Spalek, Phys. Rev. B **49**, 7898 (1994).

[19] C. Müller, A. A. Nateprov, G. Obermeier, M. Klemm, R. Tidecks, A. Wixforth, and S. Horn, J. Appl. Phys. **98**, 084111 (2005).

[20] J. H. Park, L. H. Tjeng, A. Tanaka, J. W. Allen, C. T. Chen, P. Metcalf, J. M. Honig, F. M. F. de Groot, and G. A. Sawatzky, Phys. Rev. B **61**, 11506 (2000).

[21] O. Müller, J. P. Urbach, E. Goering, T. Weber, R. Barth, H. Schuler, M. Klemm, S. Horn, and M. L. denBoer, Phys. Rev. B **56**, 15056 (1997).

[22] P. D. Dernier, J. Phys. Chem. Solids **31**, 2569 (1970).

[23] I. S. Elfimov, T. Saha-Dasgupta, and M. A. Korotin, Phys. Rev. B **68**, 113105 (2003).

[24] W. Bao, C. Broholm, G. Aeppli, P. Dai, J. M. Honig, and P. Metcalf, Phys. Rev. Lett. **78**, 507 (1997).

[25] M. S. Laad, L. Craco, and E. Müller-Hartmann, Phys. Rev. Lett. **91**, 156402 (2003).